OPEN ACCESS Freely available online

Journal of Citrus Pathology

Research Article

Two distinct viral suppressors of RNA silencing encoded by citrus tatter leaf virus

Shih-hua Tan[1], Sohrab Bodaghi[1], Arunabha Mitra[1], Stacey Comstock[1], Amy Huang[1], Sarah Hammado[1], Jinliang Liu[2], Shurooq Abu-Hajar[1], Paulina Quijia-Lamina[1], German Rafael Villalba-Salazar[1], Greg W. Douhan[1], Irene Lavagi-Craddock[1], Abigail Marie Frolli[3], Ashraf El-Kereamy[4], and Georgios Vidalakis[1]*

[1]Department of Microbiology and Plant Pathology, University of California, Riverside, California, United States of America, 92521; [2]College of Plant Sciences, Jilin University, Changchun, China, 130062; [3]University of California Agriculture and Natural Resources, Lindcove Research and Extension Center, 22963 Carson Avenue, Exeter, California, United States of America, 93221; [4]Department of Botany and Plant Sciences, University of California, Riverside, California, United States of America, 92521.

*Correspondence to: georgios.vidalakis@ucr.edu

Citation: Tan, S.; Bodaghi, S.; Mitra, A.; Comstock, S.; Huang, A.; Hammado, S., et al. (2024). Two distinct viral suppressors of RNA silencing encoded by citrus tatter leaf virus. Journal of Citrus Pathology, 11(2). http://dx.doi.org/10.5070/C411262591 Retrieved from https://escholarship.org/uc/item/30p6r1pd.

Abstract

Two proteins of the citrus tatter leaf virus (CTLV), a strain of the apple stem grooving virus (ASGV), capable of inducing citrus bud union disorders on commercially important trifoliate and citrange rootstocks, were identified as viral suppressors of RNA silencing (VSRs). Both the coat protein (CP) and the movement protein (MP) suppressed RNA silencing in GFP-transgenic *Nicotiana benthamiana* 16c plants in *Agrobacterium*-mediated co-infiltration assays; the MP acted as a local VSR, while the CP acted as a systemic VSR. When the potato virus X (PVX) infectious vector harbored either the CTLV CP or MP gene, viral infection and symptom development were promoted in *N. benthamiana*. Deletions of amino acids in the CP sequence or the MP sequence resulted in failure to promote PVX infections as well as suppression of silencing in *Agrobacterium*-mediated co-infiltration assays. Mass spectrometry-based immunoprecipitation proteomics showed that neither the CTLV CP nor the MP interacts with cellular components directly involved in host antiviral RNA silencing pathways. RNA immunoprecipitation (RIP) and RNA-protein pull-down assays indicated that the CTLV MP interacts with double-stranded RNA (dsRNA) presumably through a protein complex or proteins containing RNA binding domains. It is possible that the MP prevents dsRNA cleavage through this mechanism, leading to suppression of host antiviral RNA silencing. These findings confirm that CTLV uses VSRs as part of its overall strategy to overcome host antiviral defenses and are indicative of the ability of ASGV and CTLV to infect a wide range of hosts including different species of woody and herbaceous plants.

Keywords: VSR, *Capillovirus*, post-transcriptional gene silencing, coat protein (CP), movement protein (MP), apple stem grooving virus (ASGV)

Introduction

Citrus tatter leaf virus (CTLV) is a strain of Apple stem grooving virus, belonging to the genus *Capillovirus* in the *Betaflexiviridae* family of *Tymovirales*. Since its original discovery in California in 1962, CTLV has been reported in many citrus-producing areas worldwide (Broadbent et al. 1994; da Graca 1977; da Graca and Skaria 1996; Fraser and Broadbent 1981; Garnsey 1964, 1970; Herron and Skaria 2000; Inouye et al. 1979; Miyakawa 1980; Miyakawa and Matsui 1976; Miyakawa and Tsuji 1988; Nishio et al. 1982; Roistacher 1991; Su and Cheon 1984; Tan et al. 2019; Wallace and Drake 1962; Yoshikawa et al. 1993; Zhang and Liang 1988). CTLV can be mechanically transmitted to a wide range of woody and herbaceous hosts. No evidence of natural vector spread has been found to date, and there is very low, or no seed transmission depending on the host species (Cook et al. 2020; Inouye et al. 1979; Nishio et al. 1982; Tanner et al. 2011; Yoshikawa 2000). Stionic CTLV-infected citrus trees propagated onto trifoliate (*Poncirus trifoliata* (L.) Raf.) and trifoliate hybrid (*P. trifoliata x Citrus sinensis*) rootstocks (e.g., Carrizo and Troyer Citrange), can develop bud union crease and consequent tree decline (Calavan et al. 1963; Garnsey 1964; Roistacher 1991; Garnsey 1968). These rootstocks are used extensively by most citrus-producing countries due to their tolerance to citrus tristeza virus (CTV), which destroyed over 100 million citrus trees worldwide (Folimonova and Sun 2022; Moreno et al. 2008). The extensive use of trifoliate and trifoliate hybrid rootstocks makes CTLV a serious threat to the multi-billion-dollar citrus industry globally (Moreno et al. 2008; Roose 2014; Roose et al. 2015; Bitters 2021; Garnsey 1964; Tatineni at al. 2009; Calavan et al. 1963; Garnsey 1968).

CTLV is a single-stranded, positive-sense RNA virus with a long, rod-shaped virion, which is 600 to 650 nm long

and 13-19 nm wide (Nishio et al. 1989; Semancik and Weathers 1965). The complete genome sequences of several CTLV isolates were characterized and determined to be between 6,494 and 6,497 nucleotides (nt) (Tan et al. 2019). The genome organization of CTLV is similar to that of other capilloviruses with two overlapping open reading frames (ORFs) and a poly (A) tail at the 3′ end (Ohira et al. 1995; Tatineni et al. 2009; Yoshikawa et al. 1993). The ORF1 of CTLV encodes a putative 242-kDa polyprotein which contains a replicase coding region and a 27-kDa coat protein (CP) (Ohira et al. 1994; Ohira et al. 1995; Tatineni et al. 2009; Yoshikawa et al. 1993). ORF2 encodes a putative 36-kDa movement protein (MP) (Tatineni et al. 2009).

Plants have evolved and developed defense mechanisms designed to detect invading organisms and stop them before they are able to cause extensive damage (Ding 2010; Jones and Dangl 2006). Through small RNAs (siRNAs) associated with host RNA silencing, plants are able to regulate many biological processes including immunity against viruses and other pathogens (Baulcombe 2004; Khraiwesh et al. 2012). Viral infection in most eukaryotic hosts induces the production of virus-derived small interfering RNAs (vsiRNAs), which mediate RNA silencing resulting in specific antiviral immunity (Díaz-Pendón and Ding 2008; Ding 2010; Pumplin and Voinnet 2013; Csorba et al. 2015). In addition, the spread of the mobile silencing signals from cell-to-cell and long distance with-or-ahead of the virus can direct specific antiviral silencing, thereby inhibiting systemic infection (Díaz-Pendón and Ding 2008; Incarbone and Dunoyer 2013).

An invariable principle of the never-ending molecular arms race between viruses and hosts is the ability of viruses to avoid, actively suppress, or even hijack host defense pathways (Calil and Fontes 2016; Garcia-Ruiz 2019; Nelson and Citovsky 2005; Sanfaçon 2020; Wang et al. 2012). Therefore, successful infection requires viral proteins, which attenuate or completely inhibit the host antiviral RNA silencing pathways. These proteins are known as viral suppressors of RNA silencing (VSRs) (Burgyán and Havelda 2011; Díaz-Pendón and Ding 2008; Li and Ding 2001; Wu et al. 2010; Anandalakshmi et al. 1998). VSRs are associated with virus pathogenicity and can directly or indirectly suppress host silencing pathways and ultimately lead to enhanced virus accumulation, augmented disease symptoms, and facilitation of cell-to-cell and long-distance movement (Burgyán and Havelda 2011; Ding 2010; Díaz-Pendón and Ding 2008; Incarbone and Dunoyer 2013; Pumplin and Voinnet 2013; Csorba et al. 2015; Wu et al. 2010).

CTLV presents both an important citrus production issue as well as a fascinating virology subject. The diverse host range of this virus suggested the hypothesis that CTLV efficiently uses one or more of its proteins to suppress host antiviral RNA silencing to successfully infect and replicate in a variety of woody and herbaceous hosts. In this study, we identified and characterized two CTLV VSRs and further examined their host targets and antiviral suppression mechanisms to develop an understanding of virus-plant interactions that could lead to future solutions to CTLV-induced citrus decline on commercially important rootstocks.

Materials and Methods

Virus isolate, cloning of viral genes, microbial strains, and growth conditions

CTLV isolate TL100 was collected from Texas, USA in 1958 and maintained in a 'Meyer' lemon tree at the Rubidoux Quarantine Facility of the Citrus Clonal Protection Program (CCPP), University of California, Riverside (Tan et al. 2019). The total RNA of TL100 was extracted from 100 mg of phloem-rich bark tissue of the last matured vegetative flush (i.e., one-year-old budwood) using TRIzol™ reagent (Invitrogen™, Carlsbad, California, USA) according to the manufacturer's instructions. The total RNA was reverse-transcribed to cDNA using SuperScript™ II Reverse Transcriptase (Invitrogen™, Carlsbad, California, USA) with Oligo(dT)$_{12-18}$ primer (Invitrogen™, Carlsbad, California, USA). The CP and MP viral genes of TL100 were amplified with gene-specific primers (Supplementary Table 1) and cloned into plant expression vectors, pEarleyGate100 (pEG100; no protein tag sequence) (Earley et al. 2006) or modified pEG100 with a FLAG protein tag sequence located downstream of the coding region (pEG1001) (Supplementary Table 2). Plasmids were transformed into the *Agrobacterium tumefaciens* strain GV3101 (Wroblewski et al. 2005) and used for the transient expression of proteins in *N. benthamiana*. Both *Escherichia coli* and *A. tumefaciens* cultures were grown in Luria-Bertani (LB) liquid or agar media with the appropriate antibiotic supplements at 37°C and 28°C, respectively (Supplementary Table 2), as recommended for maintaining laboratory strains (Morton and Fuqua 2012; Tuttle et al. 2021).

Plants and growth conditions

N. benthamiana wild-type and the transgenic line 16c, which constitutively expresses green fluorescence protein (GFP) (Ruiz et al. 1998), were grown and maintained in a temperature- (20-24°C) and light- (16h light and 8h dark) controlled growth room. Plants 4 to 6 weeks old were used for the experiments. Unless otherwise specified, all experiments were performed in triplicates and repeated at least three times.

Agrobacterium-*mediated transient expression in* N. benthamiana *leaves*

The *A. tumefaciens* strain GV3101 (Wroblewski et al. 2005) carrying the desired CTLV viral gene expression constructs was used for transient expression experiments in *N. benthamiana*. *Agrobacterium* cells were resuspended in an infiltration buffer [10 mM $MgCl_2$, 10 mM 2-(N-morpholino) ethanesulfonic acid (MES), pH 5.6, and 150 µM acetosyringone] to a final OD_{600} of 0.8 to 1.0 and incubated for at least 3 hours at room temperature before infiltration (Renovell et al. 2012). Fully expanded leaves of

N. benthamiana plants at the six-leaf stage were infiltrated with a 3 mL syringe without a needle.

RNA silencing suppression in co-infiltration assays using Agrobacterium-mediated transient expression in N. benthamiana 16c plants and GFP imaging

In RNA silencing suppression co-infiltration assays, cell suspensions of the *A. tumefaciens* strain GV3101 carrying the 35S::GFP gene and *A. tumefaciens* strain GV3101 harboring the 35S::CTLV viral gene of interest were mixed in a 1 to 1 ratio to a final OD_{600} of 0.8 to 1.0 of each construct. *Agrobacterium* carrying an empty vector with no viral gene was used as a negative control.

Constructs expressing the cucumber mosaic virus (*Bromoviridae*) protein 2b (CMV-2b) and citrus leaf blotch virus (*Betaflexiviridae*) movement protein (CLBV-MP) were used as positive VSR controls (Lucy et al. 2000; Renovell et al. 2012). CMV was used as an overall assay control and CLBV as a VSR expression level control of a relative citrus virus. Fully expanded leaves of *N. benthamiana* 16c plants were infiltrated with a 3 mL syringe without a needle. To observe the gene silencing effects, the signal of GFP was visualized under a handheld long-wavelength UV lamp (Blak-Ray® Model B-100 AP, Ultraviolet Products, Upland, California, USA) at 5 days post infiltration (dpi) for local infection, and 14 dpi for systemic infection.

Northern blot hybridization of GFP mRNA and siRNA

The abundance of GFP mRNA and siRNA was examined at 5 dpi in the infiltrated leaf areas by Northern blot hybridization. Non-infiltrated systemic tissue located in the upper part of *N. benthamiana* plants was examined for GFP mRNA abundance at 14 dpi. The total RNA of each sample was extracted using TRIzol™ (Invitrogen™, Carlsbad, California, USA) per the manufacturer's instructions. RNA quality and concentration were measured with a NanoPhotometer™ (Implen, Munich, Germany), and equal amounts of RNA were loaded for blotting analysis. RNA Northern blotting was performed using the DIG Northern Starter Kit (Roche Sigma-Aldrich, St. Louis, Missouri, USA) per manufacturer's instructions. A non-radiolabeled digoxigenin (DIG)-labeled RNA probe was generated by *in vitro* transcription along with DIG-RNA labeling (Roche Sigma-Aldrich, St. Louis, Missouri, USA) which was specific and complementary to the GFP sequence. The blot was washed, developed, and further observed under a ChemiDoc™ Imaging Systems (Bio-Rad, Hercules, California, USA).

Quantification of GFP expression by reverse transcription (RT) quantitative polymerase chain reaction (qPCR)

Primers and probe for a GFP RT-qPCR assay were designed using the Primer Express™ software (Thermo Fisher Scientific, Carlsbad, California, USA). The fluorophore used for the GFP probe was 6-carboxyfluorescein (6-FAM) and the 3′ quencher was a nonfluorescent quencher (NFQ) (Supplementary Table 1). A relative standard curve was generated using 10X serial dilutions to analyze the dynamic range, precision, and efficiency of the assay. The slope of the standard curve and the coefficient of determination (R^2) were calculated using linear regression (Rasmussen 2001). Amplification efficiency (E) was calculated with the formula $E = 10^{(-1/slope)} - 1$ (Pfaffl 2001; Svec et al. 2015). An RT-qPCR assay of the *N. benthamiana* housekeeping gene protein phosphatase 2A (*NbPP2A*) (Liu et al. 2012) was also developed (Supplementary Table 1) and used as a normalizer in the quantitative gene expression analysis. The PCR reaction setup for *NbPP2A* was similar to the GFP assay except for the final concentration of each primer, which was 900 nM.

The total RNA of each sample was extracted by TRIzol™ (Invitrogen™, Carlsbad, California, USA) and treated with DNase I (New England Biolabs®, Ipswich, Massachusetts, USA) before being added to PCR reactions. The GFP RT-qPCR reaction (10 µL) was performed using the TaqMan® RNA-to-CT 1-Step Kit (Applied Biosystems, Carlsbad, California, USA) with 2.8 µL water, 5.0 µL 2X TaqMan RT-PCR Mix, 0.6 µL of each primer (600 nM as final concentration), 0.25 µL probe (250 nM as final concentration), 0.25 µL 40X TaqMan RT Enzyme Mix, and 0.5 µL of RNA (50 ng) for each reaction. The cycling conditions were 48°C for 15 minutes for the reverse transcription step, 95°C for 10 minutes during the first cycle to inactivate the RT enzyme and activate PCR polymerase, followed by 40 cycles of 95°C for 15 seconds and 60°C for 45 seconds. This assay was validated and analyzed using a QuantStudio™ 12K Flex Real-Time PCR System (Thermo Fisher Scientific, Carlsbad, California, USA). Fluorescent signals were collected during the amplification cycle, and the number of cycles required for the fluorescent signal to cross the threshold (Cq) was calculated and exported.

Relative expression levels (fold change) of the genes of interest were calculated using the Pfaffl method (Pfaffl 2001), with the buffer-treated sample as mock control (expression level of 1) and *NbPP2A* as reference gene (endogenous control). Gene expression data for the sample were averaged from three biological replicates; each biological replicate was the mean of three qPCR technical replicates. The relative expression data was analyzed and calculated by Duncan's Multiple Range Test (MRT) with significance level $\alpha = 0.05$ (Bewick et al. 2004; Tallarida and Murray 1987; Duncan 1955).

Potato virus X (PVX) assay

PCR products of CTLV-CP and -MP were digested with *Asc*I and *Not*I restriction enzymes (New England Biolabs®, Ipswich, Massachusetts, USA) and ligated into the PVX infectious clone, pGR106 (Jones et al. 1999), carrying the full PVX genome (Supplementary Table 1 and 2). Recombinant plasmids were transformed into *A. tumefaciens* strain GV3101 (pMP90::pSOUP) (Supplementary Table 2), and the resulting strains were used to infiltrate six-leaf stage wild-type *N. benthamiana* plants. The frameshift (fs) mutations of CTLV-CP and -MP were constructed using the same gene sequence but with a

few nucleotides inserted at the beginning of the reading frame.

Total RNA was extracted from samples collected at 21 dpi using TRIzol™ (Invitrogen™, Carlsbad, California, USA) and further analyzed by Northern blot hybridization as described above. The RNA probe used in Northern blotting was DIG-labeled and designed complementary to the PVX CP gene. The relative expression levels were quantified by a newly designed RT-qPCR assay targeting the PVX CP gene with the *NbPP2A* housekeeping gene used as a normalizer. The setup, validation, and analysis of the RT-qPCR were the same as described above except for the final concentration of each primer and qPCR probe, which were 600 nM and 250 nM, respectively.

CTLV-CP and -MP serial deletion mutants assayed using the PVX infectious vector pGR106

Serial deletion mutant clones were constructed using the PVX infectious vector harboring CTLV-CP (pGR106-CTLV-CP) and -MP (pGR106-CTLV-MP) with the Q5 Site-Directed Mutagenesis Kit (New England Biolabs®, Ipswich, Massachusetts, USA) per manufacturer's instructions. Primer sets for each deletion clone were designed using the NEBaseChanger® online tool (New England Biolabs® website, http://nebasechanger.neb.com/) with deletions ranging between 42 and 117 base pairs (14 to 39 amino acids) (Supplementary Table 1, 2, and Supplementary Figure 1). The deletion constructs were transformed into *A. tumefaciens* strain GV3101 (pMP90::pSOUP) (Supplementary Table 2), and the resulting strains were used to infiltrate six-leaf stage wild-type *N. benthamiana* plants. Total RNA was extracted from samples collected at 21 dpi infected with pGR106, pGR106-CTLV-CP, pGR106-CTLV-MP, and their respective deletion clones. Viral RNAs were detected and quantified using the PVX CP RT-qPCR assay with the housekeeping gene *NbPP2A* as a normalizer in the quantitative relative gene expression analysis as described above.

Protein extraction and Western blotting analysis

Total protein was extracted from 500 mg of agroinfiltrated *N. benthamiana* leaf tissue using 1 mL extraction buffer GTEN (10% [v/v] glycerol, 25 mM Tris-HCl pH 7.5, 1 mM EDTA, 150 mM NaCl) with supplements of 2% [w/v] polyvinylpolypyrrolidone (PVPP), 10 mM dithiothreitol (DTT), 0.1% Tween20, and 1X protease inhibitor cocktail for plant cell (Sigma-Aldrich, St. Louis, Missouri, USA) before use (modified from Moffett et al. 2002). The samples were mixed with the buffer by vortexing and incubated on ice for 10 minutes. Subsequently, the samples were centrifuged twice at 4°C at 15,000g for 10 minutes to remove plant debris. The supernatant was transferred to a new tube and tested by Western blotting to detect the presence of the specific proteins with a monoclonal ANTI-FLAG M2 antibody (Sigma-Aldrich, St. Louis, Missouri, USA) as primary and Anti-mouse IgG HRP-linked antibody as secondary (Cell Signaling, Danvers, Massachusetts, USA) (Supplementary Table 3).

Mass spectrometry-based immunoprecipitation (IP) proteomics

Total protein was extracted with GTEN buffer, as described above, from the *N. benthamiana* infiltrated leaves overexpressing FLAG-tagged CTLV-CP or -MP and incubated with the anti-FLAG M2 affinity gel (Sigma-Aldrich, St. Louis, Missouri, USA) overnight at 4°C with gentle agitation. The bead control was included and run in parallel. Unbound proteins were washed out five times with cold GTEN buffer (10% [v/v] glycerol, 25 mM Tris-HCl pH 7.5, 1 mM EDTA, 150 mM NaCl). Proteins bound to the anti-FLAG affinity gel were eluted using elution buffer (0.1 M glycine-HCl, pH 3.5). The IP products were analyzed by Western blotting and submitted to the IIGB Proteomics Core at the University of California, Riverside for mass spectrometry analysis. Briefly, the submitted IP products were digested using trypsin protease at 37°C overnight and then analyzed by LC-MS/MS. Both Ultraperformance Liquid Chromatography coupled with Quadrupole Time of Flight Mass Spectrometry (UPLC/QTOF-MS) and the next generation LTQ-Orbitrap Fusion LC/MS (Thermo Fisher Scientific, Carlsbad, California, USA) were used for this analysis. The protein identities of the top candidates were determined using the Mascot search engine against the *N. benthamiana* proteomic database (Boyce Thompson Institute for Plant Research, http://bti.cornell.edu/nicotiana-benthamiana/) retrieved in November 2016 (Bombarely et al. 2012). The complete set of mass spectrometry-based IP proteomics screening was repeated twice.

Sample preparation and RNA immunoprecipitation (RIP)

Leaf samples of *N. benthamiana* 16c plants were collected from the *Agrobacterium*-mediated transient expression assay after two days of co-infiltration with *Agrobacterium* strains carrying 35S::GFP and individual viral gene constructs. The total protein of each sample was extracted from 200 mg plant tissue using 1 mL phosphate buffered saline (PBS) with supplements of 0.05% Tween 20, 1 mM PMSF (Invitrogen™, Carlsbad, California, USA) and 1X protease inhibitor cocktail for plant cell (Sigma-Aldrich, St. Louis, Missouri, USA). The samples were incubated on ice for 30 minutes and mixed briefly by vortexing every 10 minutes. The samples were centrifuged twice at 4°C (15,000g for 10 minutes) to remove plant debris. The supernatant was transferred to a new tube as protein lysate for RIP assay. The RIP was conducted using the Immunoprecipitation Kit Dynabeads® Protein A (Invitrogen™, Carlsbad, California, USA) per the manufacturer's instructions. Briefly, 3.5 µg monoclonal ANTI-FLAG M2 antibody (Sigma-Aldrich, St. Louis, Missouri, USA) was added as a ligand to 35 µL magnet Dynabeads® to establish beads-antibody complex in PBS buffer plus 0.05% Tween 20 (PBST). Protein lysate was added to the complex and incubated at room temperature for 15 minutes. After incubation, the mixture was washed three times with PBST buffer. Subsequently, the target

protein and its interacting nucleic acids were eluted and further treated with Dnase I (New England Biolabs®, Ipswich, Massachusetts, USA) to remove DNA. RT-PCR analysis was carried out targeting the GFP gene using specific primers (Supplementary Table 1) and the QIAGEN OneStep RT-PCR kit (Qiagen, Hilden, Germany) per manufacturer's instructions and examined by 1.5% agarose gel electrophoresis.

In vitro transcription of double stranded (ds) and small interfering (si) RNAs

dsRNA of GFP was transcribed using the MEGAscript® RNAi Kit (Invitrogen™, Carlsbad, California, USA) per manufacturer's instructions. The plasmids were digested either with *Mlu*I or *Nco*I restriction enzymes (New England Biolabs®, Ipswich, Massachusetts, USA) to linearize the plasmid and use as a template for *in vitro* transcription. The T7 promoter was incorporated either upstream or downstream of the GFP sequence (Supplementary Table 2) for the T7 RNA polymerase to transcribe into sense or antisense GFP RNA. The reaction contained 5 µg of linear DNA template, 2 µL 10X T7 reaction buffer, 2 µL of each 75 mM ATP/CTP/GTP/UTP solution, 2 µL T7 enzyme mix, and adjusted with nuclease-free water to 20 µL. The reactions were incubated at 37°C for 4 hours. Subsequently, both GFP transcripts were mixed (1:1 ratio), heated at 75°C for 5 minutes and left on the bench to cool down to room temperature. This allowed sense and antisense GFP to anneal and form dsRNA. siRNAs of GFP were prepared by digesting GFP dsRNA with *E. coli* Rnase III (Applied Biosystem, Carlsbad, California, USA), and further purified by running the reaction through an Amicon® Ultra-0.5 centrifuge filter unit (Millipore Sigma, Burlington, Massachusetts, USA), collecting the flow-through containing 15-30 bp siRNAs.

RNA-protein pull-down assay

The *in vitro* transcribed dsRNA and siRNA of GFP were labeled with a single biotinylated nucleotide to the 3′ terminus using Pierce™ RNA 3′ End Desthiobiotinylation Kit (Thermo Fisher Scientific, Carlsbad, California, USA). The labeled RNA was used in an RNA-protein pull-down assay using Pierce™ Magnetic RNA-Protein Pull-Down Kit (Thermo Fisher Scientific, Carlsbad, California, USA) per manufacturer's instructions. The labeled RNA (50 pmol), either dsRNA or siRNA, was captured by streptavidin magnetic beads (50 µL). Protein lysate (60 µL) extracted by GTEN buffer as described above was added to the beads-RNA complex along with 10 µL 10X protein-RNA binding buffer and 30 µL 50% glycerol. The reactions were incubated at 4°C for 60 minutes with gentle agitation followed by wash and elution steps. The eluate was examined by Western blot analysis as described above. The inputs of protein samples were also checked by Western blot analysis, and the dsRNA and siRNA species were examined by 10% and 15% polyacrylamide gel electrophoresis, respectively.

Results

CTLV-CP and CTLV-MP are systemic and local VSRs, respectively

The two highly conserved CTLV genes, CP and MP, were selected as VSR candidates, based on a previous study of various CTLV genome sequences (Tan et al. 2019). The CTLV CP and MP were cloned individually in *35S*-based plant expression binary vectors. Expression of both CTLV clones as well as the VSR positive control clones (CMV-2b and CLBV-MP), led to synthesis of their respective encoded proteins in agroinfiltrated *N. benthamiana* leaves while the empty vector control expressed no proteins as demonstrated by Western blotting analysis (Figure 1a).

The VSR positive controls CMV-2b and CLBV-MP suppressed both local and systemic RNA silencing as the GFP fluorescence signal was evident under UV light in both agroinfiltrated and non-infiltrated upper/systemic leaves (Figure 1b and Table 1). Expression of CTLV-CP resulted in a pattern similar to that obtained from the empty vector control, that is, the GFP fluorescence signal did not express locally (Figure 1b and Table 1). On the other hand, the CTLV-MP co-infiltration area expressed GFP signal and had local suppression of RNA silencing at 5 dpi with 46% suppression rate, similar to the CLBV-MP (41%) but less than CMV-2b (100%) controls (Figure 1b and Table 1).

Table 1. GFP silencing suppression rates from co-infiltration assays in *Nicotiana benthamiana* 16c plants with CTLV-CP and -MP.

Constructs	No. of Plants Infiltrated	No. of Plants Silencing Suppressed	
		Locally (5 dpi)	Systemically (14 dpi)
pEG100-GFP + pEG100	40	0 **(0%)**	0 **(0%)**
pEG100-GFP + pEG100-CMV-2b	40	40 **(100%)**	40 **(100%)**
pEG100-GFP + pEG100-CTLV-CP	39	0 **(0%)**	17 **(44%)**
pEG100-GFP + pEG100-CTLV-MP	39	18 **(46%)**	0 **(0%)**
pEG100-GFP + pEG100-CLBV-MP	39	16 **(41%)**	6 **(15%)**

Observation of non-infiltrated systemic leaves at 14 dpi showed that CTLV-CP induced a higher silencing suppression rate (44%) than that of the CLBV-MP (15%) and lower than that of the CMV-2b (100%) control (Figure

1b and Table 1). CTLV-MP did not display any systemic suppression in non-infiltrated leaves (Figure 1b and Table 1).

The abundance of GFP mRNA and GFP siRNA was examined by Northern blot hybridization to confirm the suppression of RNA silencing. Northern blot hybridization was conducted using DIG-labeled RNA probes targeting the positive strand of GFP RNA. In the infiltrated leaf areas, the empty vector control and CTLV-CP showed reduced or no GFP mRNA accumulation with an increased abundance of GFP siRNA (Figure 1c; local). In contrast, leaves co-infiltrated with GFP and CMV-2b, CLBV-MP or CTLV-MP strongly reduced the abundance of GFP siRNA, leading to increased accumulation of GFP transcripts (Figure 1c; local).

Both empty vector and CTLV-MP showed lower abundance in GFP transcripts in non-inoculated tissues (Figure 1c; systemic). However, CMV-2b, CLBV-MP, and CTLV-CP suppressed the systemic silencing of GFP with higher GFP mRNA accumulation (Figure 1c; systemic). Taken together, these results confirmed that CTLV has two VSRs. The CTLV MP appeared to have a suppression activity in local RNA silencing, while the CTLV CP interfered with RNA silencing systemically.

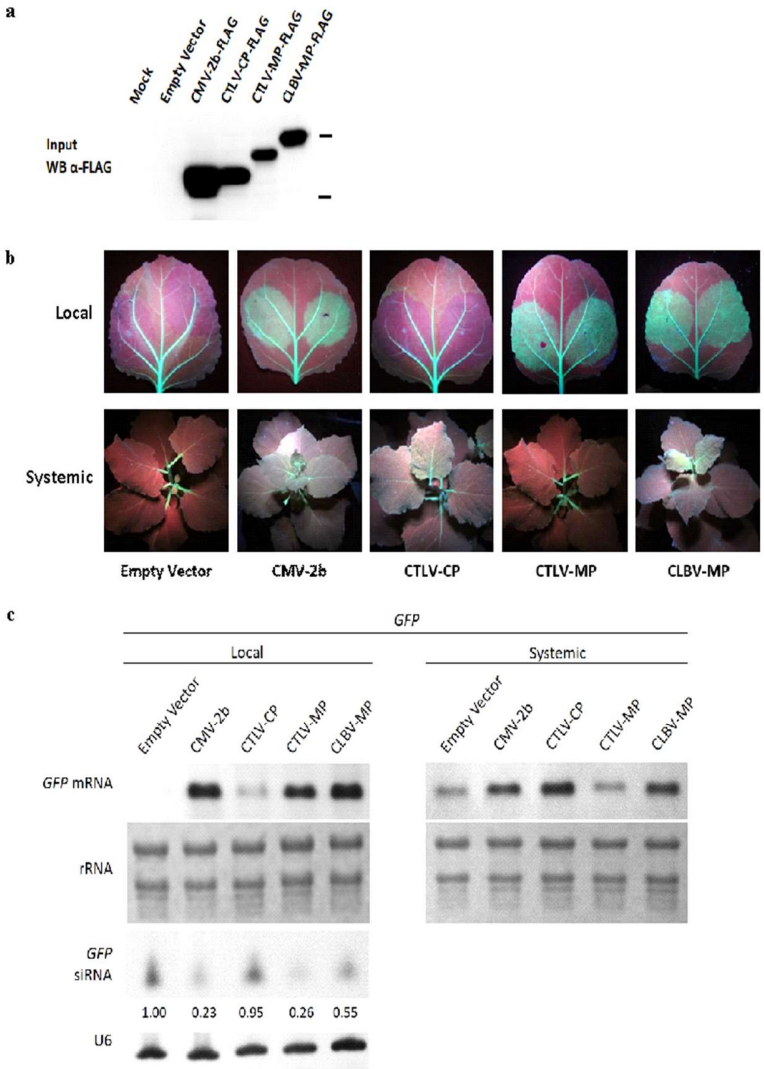

Fig. 1. RNA silencing suppression co-infiltration assay of CTLV coat protein and movement protein. Empty vector was used as negative control and CMV-2b and CLBV-MP were used as positive controls of viral suppressor of RNA silencing. (a) Western blot analysis to confirm protein expression. (b) Local (upper row) and systemic (lower row) silencing suppression observed under UV light at 5 and 14 dpi, respectively in *Nicotiana benthamiana* 16c plants. (c) Northern blot analysis for testing *GFP* mRNA level. siRNA of GFP was also examined for local infiltrated tissue. Number represents the intensity of signal compared to empty vector. Ribosomal RNA and U6 snRNA were used as loading controls. (WB: western blot; CMV-2b: cucumber mosaic virus 2b; CTLV: citrus tatter leaf virus; CLBV: citrus leaf blotch virus; CP: coat protein; MP: movement protein; rRNA: ribosomal RNA)

To quantify the relative gene expression level of GFP in each sample, RT-qPCR assays for GFP and one endogenous *N. benthamiana* gene control, *NbPP2A*, were designed and validated. The GFP RT-qPCR assay had a linear dynamic range with R^2 equal to 0.9999 and 102.1% efficiency (Figure 2a). The *NbPP2A* RT-qPCR also

showed a linear dynamic range with R^2 equal to 0.9996 and 103.3% as its efficiency (Figure 2b).

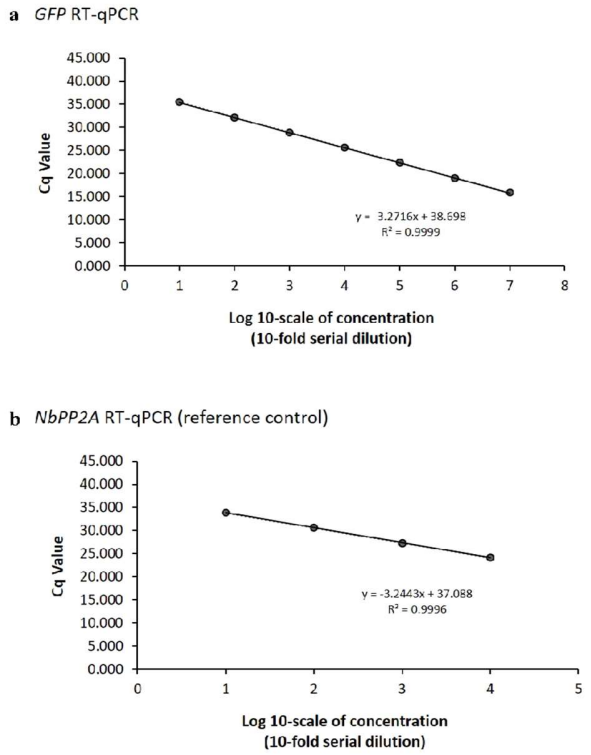

Fig. 2. Standard curve analysis for validation of RT-qPCR assays. The X-axis displays the log concentration and the Y-axis represents the value of quantitative cycle (Cq). (a) *GFP* RT-qPCR assay. (b) *NbPP2A* RT-qPCR assay.

Relative expression analysis showed that CMV-2b, CLBV-MP, and CTLV-MP had significantly higher GFP expression levels than the empty vector control in local and infiltrated leaves ($\alpha = 0.05$; Figure 3a). In upper and non-infiltrated leaves, CMV-2b, CLBV-MP, and CTLV-CP had significantly higher GFP expression levels than the empty vector control ($\alpha = 0.05$; Figure 3b). CTLV-MP also had statistically higher GFP expression than the empty vector in this case; however, the levels of expression were equal to or more than 50% lower than those of the VSR controls and that of CTLV-CP. The GFP expression level results were consistent with the UV-light visual observations and Northern blot analysis, and further supported the hypothesis that the CTLV CP and MP are VSRs.

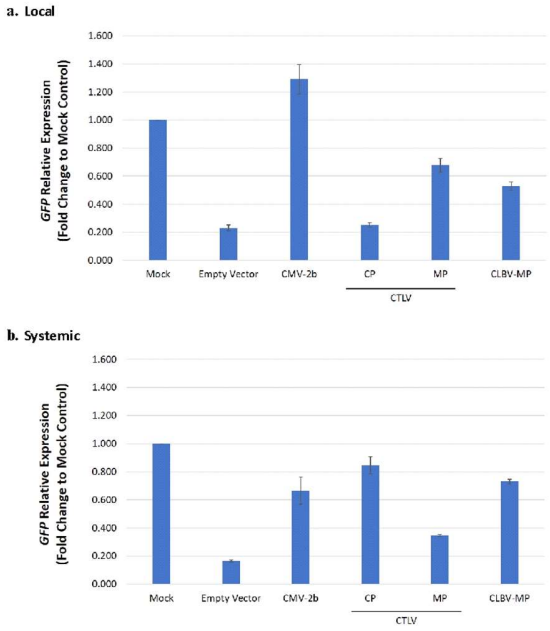

Fig. 3. Relative expression analysis of GFP mRNA for silencing suppression co-infiltration assay in *Nicotiana benthamiana* 16c plants. (a) Local infiltrated leaf tissue collected at 5 dpi. (b) Systemic tissue collected at 14 dpi. The experiments were performed in triplicates and repeated at least three times (Significance level $\alpha = 0.05$). Vertical lines on the bars indicate standard deviation. (CMV-2b: cucumber mosaic virus; CTLV: citrus tatter leaf virus; CLBV: citrus leaf blotch virus; CP: coat protein; MP: movement protein)

PVX-CTLV-CP and PVX-CTLV-MP induced severe symptoms and accumulated to high levels in N. benthamiana

To test whether the CTLV CP and MP are capable of suppressing siRNA-mediated host immunity, CTLV-CP and CTLV-MP were introduced individually into the PVX infectious clone, pGR106, and their effect on viral virulence was examined at 21 dpi. Unlike *N. benthamiana* plants infected with wild-type PVX (pGR106 without CTLV-CP/MP insertions), plants infected with PVX harboring either CTLV-CP (PVX-CTLV-CP) or -MP (PVX-CTLV-MP) showed severe mosaic and leaf deformation symptoms on newly emerged leaves along the apical shoots, similar to the PVX-CLBV-MP control (Figure 4a). Consistent with the observed enhanced virulence, Northern blot analysis demonstrated that viral RNAs accumulated to a much higher level in PVX-CTLV-CP infected tissues compared to the wild-type PVX (Figure 4b). PVX-CTLV-MP also enhanced *N. benthamiana* symptoms and PVX RNA accumulation (Figure 4b), though to a lesser extent than the PVX-CTLV-CP.

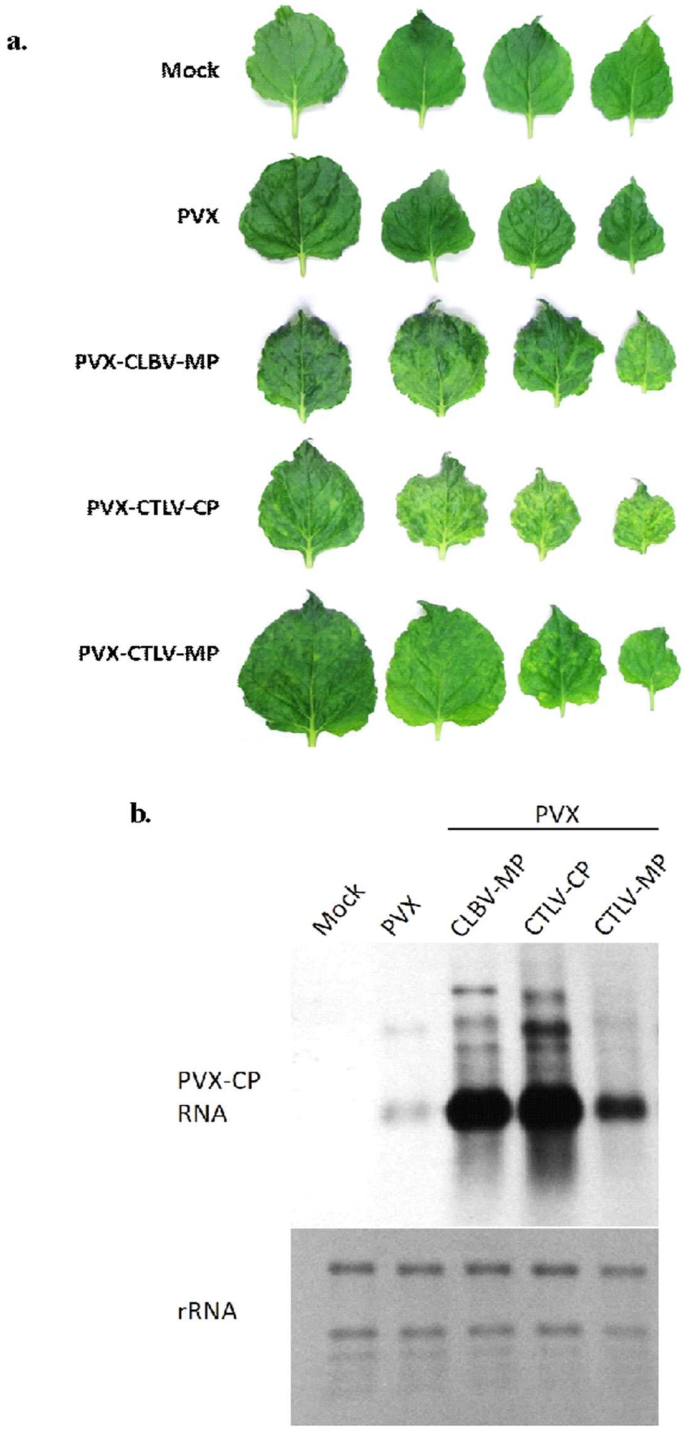

Fig. 4. PVX assay to test the CTLV-CP and -MP for suppression of siRNA-mediated host immunity in *N. benthamiana* plants. (a) Leaf symptoms. (b) Northern blot analysis with DIG-labeled PVX coat protein sgRNA-targeting probe to detect viral accumulation. Ribosomal RNA was stained and visualized as the loading control. The experiments were performed in triplicates and repeated at least three times. (PVX: potato virus X; CLBV: citrus leaf blotch virus; CTLV: citrus tatter leaf virus; CP: coat protein; MP: movement protein)

The relative PVX gene expression levels were quantified in each sample using the newly designed and validated RT-qPCR assays targeting the PVX CP gene and the *N. benthamiana NbPP2A* gene, which was used as the endogenous plant gene control. The PVX CP RT-qPCR assay validation showed a linear dynamic range with R^2 equal to 0.9998 and 100.1% as its efficiency (Figure 5a) while the *NbPP2A* performed as previously described (Figure 2b).

PVX-CTLV-CP and PVX-CTLV-MP infected tissues had nearly 25-fold and 10-fold increases in PVX RNA loads relative to the wild-type PVX infectious clone, respectively (significance level α = 0.05; Figure 5b). In addition, frameshift mutation controls of the PVX-CTLV-CP and -MP exhibited mild or no mosaic symptoms and similar fold change of the virus RNA load in comparison to the wild-type PVX (Figure 5b and 5c).

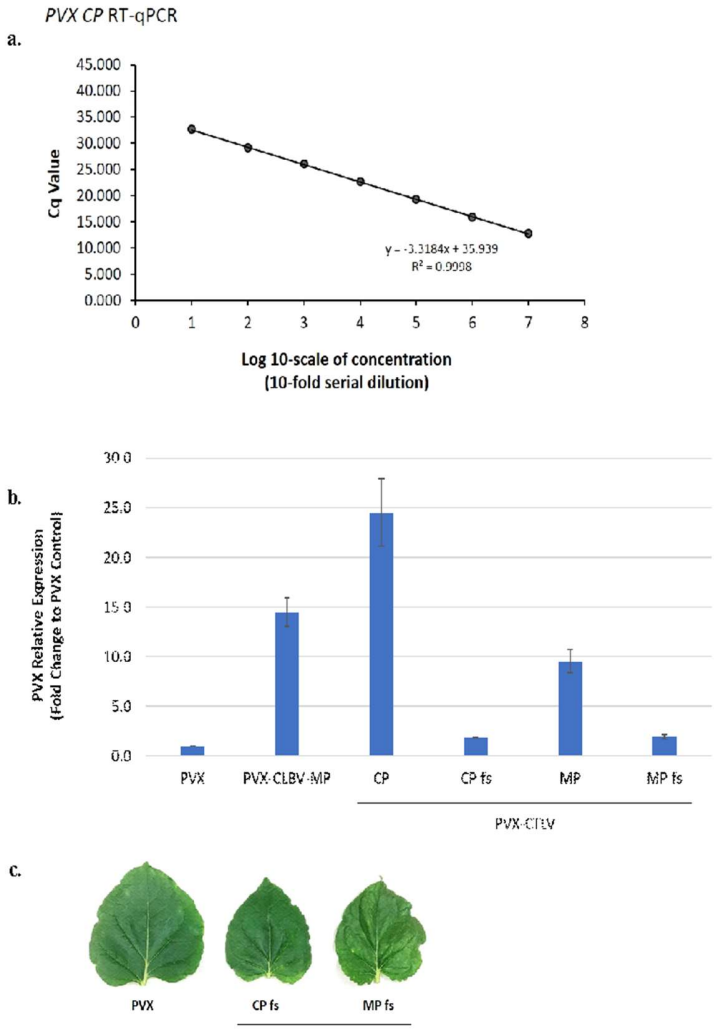

Fig. 5. PVX assay to test CTLV-CP, -MP, and their frameshifting mutations on the suppression of siRNA-mediated host immunity in *N. benthamiana* plants. (a) Standard curve analysis to validate the RT-qPCR assay targeting the PVX CP gene. The X-axis displays the log concentration and the Y-axis represents the value of quantitative cycle (Cq). (b) Relative expression levels from the PVX-CP-targeting RT-qPCR assay. Vertical lines on the bars indicate standard deviation. (Significance level α = 0.05). (c) Leaf symptoms induced by frameshifting mutations of CTLV-CP and -MP. The experiments were performed in triplicates and repeated at least three times. (PVX: potato virus X; CLBV: citrus leaf blotch virus; CTLV: citrus tatter leaf virus; CP: coat protein; MP: movement protein; fs: frameshifting mutation)

PVX-CTLV-CP$^{\Delta 36\text{-}70}$ cannot promote symptom development and viral accumulation

To identify the CTLV CP regions associated with the host silencing suppression function, clones with serial deletions (Supplementary Figure 1a) were constructed in the PVX infectious vector and agroinfiltrated into wild-type *N. benthamiana*. The newly emerged leaves along the apical shoots were observed at 21 dpi. Among the PVX-CTLV-CP deletion clones, leaves infected with PVX-CTLV-CP$^{\Delta 36\text{-}70}$ (D2) did not show mosaic symptoms, and the observed leaf deformations were similar to the leaves infected with the wild-type PVX (Figure 6a). Symptom development of all other deletion clones was similar to the PVX-CTLV-CP (Figure 6a). Quantitative analysis also showed that CTLV-CP$^{\Delta 36\text{-}70}$ (D2) had the lowest PVX RNA accumulation (Figure 6b; significance level α = 0.05). This indicated that the functional region of the CTLV CP associated with the silencing suppression activity is located in the 36-70 amino acid region.

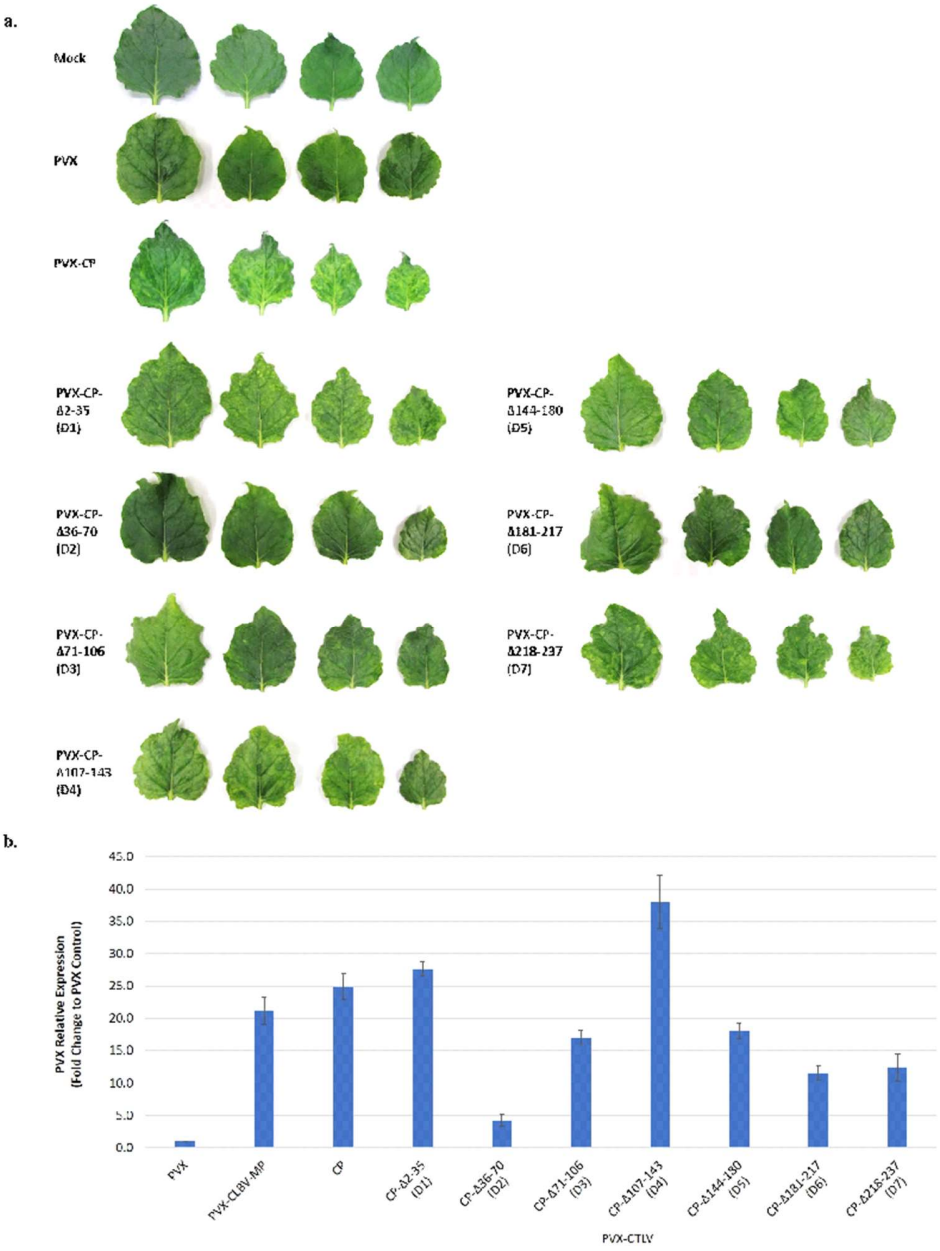

Fig. 6. CTLV-CP serial deletion mutants built using the PVX infectious vector to identify regions associated with VSR activity in wild-type *N. benthamiana* plants. (a) Leaf symptoms of CTLV-CP and its deletion mutants. (b) Relative expression levels of CTLV-CP and its deletion mutants by the PVX-CP-targeting RT-qPCR assay (Significance level $\alpha = 0.05$). Vertical lines on the bars indicate standard deviation. The experiments were performed in triplicates and repeated at least three times. (PVX: potato virus X; CLBV: citrus leaf blotch virus; CTLV: citrus tatter leaf virus; CP: coat protein; MP: movement protein)

PVX infectious vector expressing CTLV-MP$^{\Delta 112\text{-}143}$ cannot promote symptom development and viral accumulation

To identify the CTLV MP regions associated with the host silencing suppression function, clones with serial deletions (Supplementary Figure 1b) were constructed in the PVX infectious vector and agroinfiltrated into wild type *N. benthamiana*. Newly emerged leaves along the apical shoots were observed at 21 dpi. Among the PVX-CTLV-MP deletion clones, leaves infected with PVX-CTLV-MP$^{\Delta 112\text{-}143}$ (D4) did not show mosaic symptoms, and leaf deformations were similar to the leaves infected with the wild-type PVX (Figure 7a). The development of symptoms in response to the expression of all other PVX-CTLV-MP deletion clones was similar to that observed with the full-length PVX-CTLV-MP (Figure 7a). Quantitative analysis also showed that CTLV-MP$^{\Delta 112\text{-}143}$ (D4) had the lowest PVX RNA accumulation (Figure 7b; significance level $\alpha = 0.05$). This indicated that the functional region associated with the silencing suppression activity of the CTLV MP is located within the 112 and 143 amino acid regions.

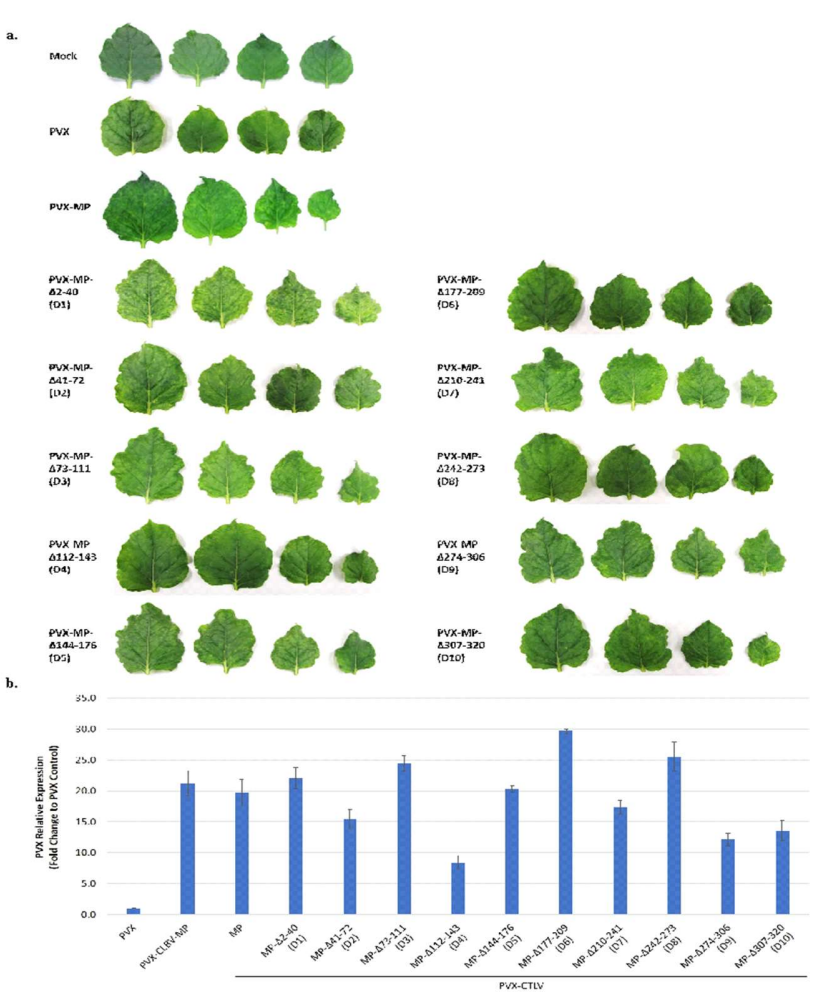

Fig. 7. CTLV-MP serial deletion mutants built using the PVX infectious vector to identify regions associated with VSR activity in wild-type *N. benthamiana* plants. (a) Leaf symptoms of CTLV-MP and its deletion mutants. (b) Relative expression levels of CTLV-MP and its deletion mutants by the PVX-CP-targeting RT-qPCR assay (Significance level $\alpha = 0.05$). Vertical lines on the bars indicate standard deviation. The experiments were performed in triplicates and repeated at least three times. (PVX: potato virus X; CLBV: citrus leaf blotch virus; CTLV: citrus tatter leaf virus; MP: movement protein)

CTLV-CP$^{\Delta 36\text{-}70}$ and -MP$^{\Delta 112\text{-}143}$ do not exhibit silencing suppression activity

To confirm the functional regions of the CTLV CP and MP associated with host RNA silencing suppression, *Agrobacterium*-mediated transient expression experiments were performed with the GFP-expressing vector and CTLV-CP$^{\Delta 36\text{-}70}$ (D2) and CTLV-MP$^{\Delta 112\text{-}143}$ (D4) co-infiltrated into *N. benthamiana* 16c plants.

The protein expression levels of CTLV-CP$^{\Delta 36\text{-}70}$ and CTLV-MP$^{\Delta 112\text{-}143}$ were confirmed by Western blot analysis (Figure 8a). The CTLV-CP-infiltrated plants co-infiltrated with GFP were observed at 14 dpi under UV light; GFP signal was observed in non-infiltrated upper leaves. In contrast, plants co-infiltrated with GFP and CTLV-CP$^{\Delta 36\text{-}70}$ showed an absence of or low GFP signal, indicating loss of CTLV-CP's systemic silencing suppression activity (Figure 8b; systemic).

When the plants co-infiltrated with GFP and CTLV-MP were observed at 5 dpi under UV light, the GFP signal was observed in the local infiltrated areas (Figure 1b and 8b; local). Plants co-infiltrated with GFP and CTLV-MP$^{\Delta 112\text{-}143}$ showed no or low GFP signal, indicating loss of CTLV-MP's local silencing suppression activity (Figure 8b; local).

The suppression rate of both CTLV-CP$^{\Delta 36\text{-}70}$ and CTLV-MP$^{\Delta 112\text{-}143}$ were decreased (Table 2) as shown by quantitative analysis, consistently with the UV light observations. The local leaves infiltrated with CTLV-MP$^{\Delta 112\text{-}143}$ had significantly lower GFP expression than the wild-type CTLV MP ($\alpha = 0.05$; Figure 8c) at 5 dpi. Similarly, new leaves above the infiltration site infiltrated with CTLV-CP$^{\Delta 36\text{-}70}$ had significantly lower GFP expression than wild-type CTLV-CP ($\alpha = 0.05$; Figure 8d) at 14 dpi. These results further supported the hypothesis that both CTLV-CP$^{\Delta 36\text{-}70}$ and CTLV-MP$^{\Delta 112\text{-}143}$ do not have suppression activity, indicating the respective deletion mutations affect their functional regions associated with host RNA silencing suppression.

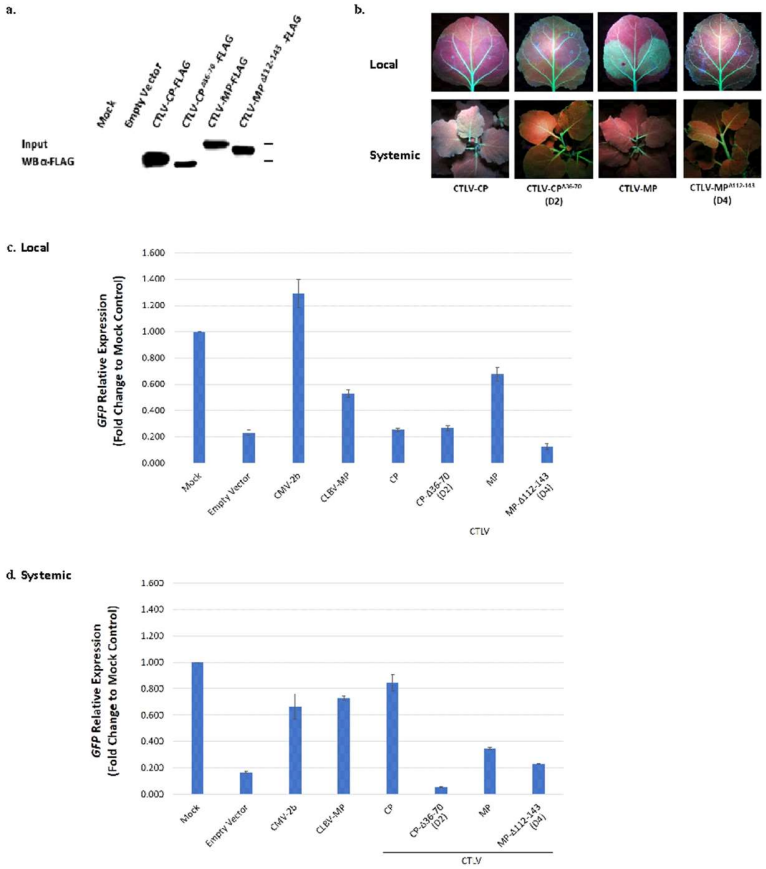

Fig. 8. RNA silencing suppression co-infiltration assay of CTLV-CP, -MP, and their deletion mutants in *N. benthamiana* 16c plants. (a) Western blot analysis to confirm protein expression. (b) Local (upper row) and systemic (lower row) silencing suppression observed under UV light at 5 and 14 dpi, respectively. Relative expression level analysis for *GFP* mRNA levels in both (c) local tissue and (d) systemic tissues by the *GFP*-targeting RT-qPCR assay (Significance level $\alpha = 0.05$). Vertical lines on the bars indicate standard deviation. The experiments were performed in triplicates and repeated at least three times. (WB: western blot; CMV-2b: cucumber mosaic virus 2b; CLBV: citrus leaf blotch virus; CTLV: citrus tatter leaf virus; CP: coat protein; MP: movement protein)

Table 2. GFP silencing suppression rates from co-infiltration assays in *Nicotiana benthamiana* 16c plants with CTLV-CP and -MP carrying partial deletions.

Constructs	No. of Plants Infiltrated	No. of Plants Silencing Suppressed	
		Locally (5 dpi)	Systemically (14 dpi)
pEG100-GFP + pEG100-CTLV-CP	39	0 **(0%)**	17 **(44%)**
pEG100-GFP + pEG100-CTLV-CP$^{\Delta 36\text{-}70}$ (D2)	12	0 **(0%)**	2 **(17%)**
pEG100-GFP + pEG100-CTLV-MP	39	18 **(46%)**	0 **(0%)**
pEG100-GFP + pEG100-CTLV-MP$^{\Delta 122\text{-}143}$ (D4)	12	2 **(17%)**	0 **(0%)**

CTLV-CP and CTLV-MP did not directly interact with major host cellular proteins in the RNA silencing pathway

To identify the CTLV CP- and MP-associated host proteins, immunoprecipitation products were analyzed by mass spectrometry. Both CTLV-CP and CTLV-MP generated long lists of candidate plant proteins. The exponentially modified protein abundance index (emPAI, set at ≥1) was used to filter the data based on the abundances of the proteins interacting with either the CTLV CP or the CTLV MP so that a total of 100 protein hits were found in the CTLV-CP-expressing samples but not in the control (Table 3 and Supplementary Table 4).

For the CTLV-MP-expressing samples, a total of 98 protein hits were found (Table 4 and Supplementary Table 5). However, none of the major protein components of the plant RNA silencing pathway was identified in either the CTLV CP (Table 3 and Supplementary Table 4) or the CTLV MP (Table 4 and Supplementary Table 5) expressing samples. These results indicated that the CTLV CP and MP do not suppress host antiviral RNA silencing

through a direct interaction with the protein components of the pathway.

Table 3. List of the top 30 potential CTLV-CP-associated host proteins identified by UPLC/Q-TOF-MS in *N. benthamiana*.

No.	*N. benthamiana* Accession No.**	Best Match in *Arabidopsis thaliana*	Protein Name / Description*	No. of Observed Peptides	emPAI	Mascot Score	Sequence Coverage
1	NbS00035989g0001.1	AT5G11580.1	Regulator of chromosome condensation (RCC1) family protein	21	26.12	777.08	37.80
2	NbS00027424g0009.1	AT1G09620.1	ATP binding/leucine-tRNA ligases/aminoacyl-tRNA ligase	48	11.83	1105.95	51.46
3	NbS00000088g0002.1	AT4G30010.1	ATP-dependent RNA helicase	2	9.00	23.15	20.93
4	NbS00019288g0006.1	AT5G23860.2	beta-tubulin	7	7.58	416.60	30.00
5	NbS00030810g0011.1	AT2G43160.1	ENTH/VHS family protein	17	7.11	454.54	26.11
6	NbS00003947g0013.1	AT5G64460.8	Phosphoglycerate mutase family protein	7	6.74	36.46	66.91
7	NbS00031412g0004.1	AT3G12110.1	Actin-11, ACT11	12	6.11	520.46	39.43
8	NbS00006458g0003.1	AT4G14960.2	alpha-tubulin isoform, TUA6	14	5.72	575.98	38.80
9	NbS00000030g0010.1	AT2G43160.4	ENTH/VHS family protein	17	5.66	437.14	20.02
10	NbS00044990g0002.1	AT2G39730.1	Rubisco activase, RCA	18	5.58	505.23	50.56
11	NbS00016397g0010.1	AT4G33090.1	Puromycin-sensitive aminopeptidase	31	5.56	485.22	45.77
12	NbS00046182g0007.1	AT5G59370.2	Actin 4	10	4.75	464.42	40.05
13	NbS00003962g0006.1	AT2G37370.1	Centrosomal protein of 135 kDa-like protein	13	4.62	164.01	52.91
14	NbS00027242g0004.1	AT5G59613.2	ATP synthase	2	4.62	13.32	31.34
15	NbS00003508g0016.1	AT3G13330.1	Proteasome activating protein 200	50	4.01	1034.15	37.56
16	NbS00019252g0009.1	AT3G20320.1	Trigalactosyldiacylglycerol2	6	3.92	50.49	28.72
17	NbS00002899g0003.1	AT1G04430.2	S-adenosyl-L-methionine-dependent methyltransferases superfamily protein	23	3.81	274.80	41.42
18	NbS00022532g0009.1	AT3G20320.1	Trigalactosyldiacylglycerol2	13	3.77	358.42	38.92
19	NbS00004706g0011.1	AT3G18480.1	CCAAT-displacement protein alternatively spliced product	22	3.73	179.03	38.15
20	NbS00054890g0003.1	AT4G00430.1	Plasma membrane intrinsic protein 1	9	3.64	54.18	41.81
21	NbS00003552g0008.1	AT3G18480.1	CCAAT-displacement protein alternatively spliced product	32	3.53	344.14	38.61
22	NbS00008003g0012.1	AT3G18480.1	CCAAT-displacement protein alternatively spliced product	32	3.53	322.91	43.87
23	NbS00057125g0003.1	AT1G04430.2	S-adenosyl-L-methionine-dependent methyltransferases superfamily protein	22	3.49	274.34	37.50
24	NbS00030134g0011.1	AT5G09880.1	Splicing factor, CC1-like	13	3.42	165.19	27.15
25	NbS00016385g0017.1	AT3G18480.1	CCAAT-displacement protein alternatively spliced product	30	3.24	254.68	41.60
26	NbS00006841g0003.1	AT4G00430.1	Plasma membrane intrinsic protein 1	9	3.22	56.87	41.81
27	NbS00003479g0020.1	AT5G54160.1	O-methyltransferase 1	8	3.22	96.88	30.58
28	NbS00045109g0006.1	AT5G54160.1	O-methyltransferase 1	7	3.06	100.14	30.58
29	NbS00003172g0001.1	AT3G23820.1	UDP-D-glucuronate 4-epimerase 6	13	3.05	145.85	37.11
30	NbS00043286g0001.1	AT1G65980.1	Thioredoxin-dependent peroxidase 1	2	2.98	27.69	16.67

*The mass spectrometry-based IP proteomics screening was repeated twice for CTLV-CP.
**The *N. benthamiana* proteomic database was retrieved in November 2016 from Boyce Thompson Institute for Plant Research, (http://bti.cornell.edu/nicotiana-benthamiana/) (Bombarely et al. 2012).

Table 4. List of the top 30 potential CTLV-MP-associated host proteins identified by UPLC/Q-TOF-MS in *N. benthamiana*.

No.	*N. benthamiana* Accession No.**	Best Match in *Arabidopsis thaliana*	Protein Name / Description*	No. of Observed Peptides	emPAI	Mascot Score	Sequence Coverage
1	NbS00035989g0001.1	AT5G11580.1	Regulator of chromosome condensation (RCC1) family protein	21	26.12	777.08	37.80
2	NbS00056603g0002.1	AT1G75780.1	Tubulin beta-1 chain, TUB1	12	17.33	588.10	39.67
3	NbS00027424g0009.1	AT1G09620.1	ATP binding; leucine-tRNA ligases; aminoacyl-tRNA ligases; nucleotide binding	48	11.83	1105.95	51.46
4	NbS00030497g0004.1	AT5G23860.2	Tubulin beta 8, TUB8	8	10.66	428.48	27.81
5	NbS00000088g0002.1	AT4G30010.1	ATP-dependent RNA helicase	2	9.00	23.15	20.93
6	NbS00030810g0011.1	AT2G43160.1	ENTH/VHS family protein	17	7.11	454.54	26.11
7	NbS00003947g0013.1	AT5G64460.8	Phosphoglycerate mutase family protein	7	6.74	36.46	66.91
8	NbS00008911g0002.1	AT1G42970.1	Glyceraldehyde-3-phosphate dehydrogenase B subunit	19	5.66	639.11	46.28
9	NbS00000030g0010.1	AT2G43160.4	ENTH/VHS family protein	17	5.66	437.14	20.02
10	NbS00016397g0010.1	AT4G33090.1	Aminopeptidase M1	31	5.56	485.22	45.77
11	NbS00045823g0014.1	AT2G28900.1	Outer plastid envelope protein 16-1	4	4.62	27.36	47.77
12	NbS00003962g0006.1	AT5G13560.1	Structural maintenance of chromosomes protein	13	4.62	164.01	52.91
13	NbS00003508g0016.1	AT3G13330.1	Proteasome activating protein 200	50	4.01	1034.15	37.56
14	NbS00019252g0009.1	AT3G20320.1	Trigalactosyldiacylglycerol2	6	3.92	50.49	28.72
15	NbS00002899g0003.1	AT1G04430.2	S-adenosyl-L-methionine-dependent methyltransferases superfamily protein	23	3.81	274.80	41.42
16	NbS00022532g0009.1	AT3G20320.1	Trigalactosyldiacylglycerol2	13	3.77	358.42	38.92
17	NbS00004706g0011.1	AT3G18480.1	CCAAT-displacement protein alternatively spliced product	22	3.73	179.03	38.15
18	NbS00054890g0003.1	AT4G00430.1	Plasma membrane intrinsic protein 1	9	3.64	54.18	41.81
19	NbS00003552g0008.1	AT3G18480.1	CCAAT-displacement protein alternatively spliced product	32	3.53	344.14	38.61
20	NbS00008003g0012.1	AT3G18480.1	CCAAT-displacement protein alternatively spliced product	32	3.53	322.91	43.87
21	NbS00057125g0003.1	AT1G04430.2	S-adenosyl-L-methionine-dependent methyltransferases superfamily protein	22	3.49	274.34	37.50
22	NbS00030134g0011.1	AT5G09880.1	Splicing factor, CC1-like	13	3.42	165.19	27.15
23	NbS00016385g0017.1	AT3G18480.1	CCAAT-displacement protein alternatively spliced product	30	3.24	254.68	41.60
24	NbS00006841g0003.1	AT4G00430.1	Plasma membrane intrinsic protein 1	9	3.22	56.87	41.81
25	NbS00016445g0012.1	AT5G09810.1	Actin 7	8	3.22	317.00	35.16
26	NbS00003479g0020.1	AT5G54160.1	O-methyltransferase 1	8	3.22	96.88	30.58
27	NbS00045109g0006.1	AT5G54160.1	O-methyltransferase 1	7	3.06	100.14	30.58
28	NbS00003172g0001.1	AT3G23820.1	UDP-D-glucuronate 4-epimerase 6	13	3.05	145.85	37.11
29	NbS00021129g0002.1	AT4G30010.1	ATP-dependent RNA helicase	1	2.98	11.97	18.60
30	NbS00043286g0001.1	AT1G65980.1	Thioredoxin-dependent peroxidase 1	2	2.98	27.69	16.67

*The mass spectrometry-based IP proteomics screening was repeated twice for CTLV-MP.

**The *N. benthamiana* proteomic database was retrieved in November 2016 from Boyce Thompson Institute for Plant Research, (http://bti.cornell.edu/nicotiana-benthamiana/) (Bombarely et al. 2012).

CTLV-MP interacts with dsRNA of GFP

To investigate whether the CTLV CP and MP interact with dsRNA, RNA immunoprecipitation (RIP) experiments were conducted using *Agrobacterium*-based transient expression assays. The identified CTLV VSRs (CTLV-CP and CTLV-MP) were co-infiltrated with GFP expressing vectors in *N. benthamiana* 16c plants, where host silencing was induced and GFP dsRNA was formed *in planta*. The turnip crinkle virus (TCV) P38 protein, previously shown to interact with long dsRNAs to suppress host RNA silencing, was used as a VSR positive control (Incarbone and Dunoyer 2013; Mérai et al. 2006).

The RIP experiments revealed that the GFP dsRNA was precipitated along with the CTLV MP and the TCV P38 (Figure 9). In addition, the deletion clone CTLV-MP$^{\Delta 112\text{-}143}$, did not display a dsRNA binding ability (Figure 9). CTLV-CP did not show any interaction with dsRNA (Figure 9).

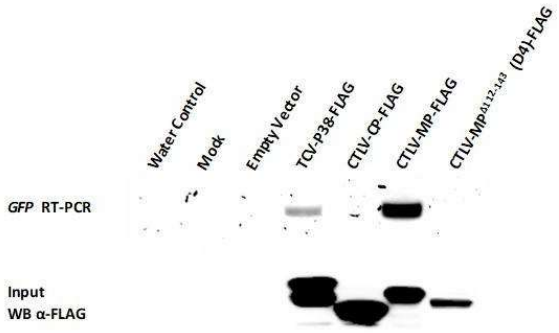

Fig. 9. RNA immunoprecipitation (RIP) of CTLV-CP, -MP, and the CTLV-MP deletion mutant. The agarose gel electrophoresis of *GFP* RT-PCR products is shown in the upper panel. The protein input was examined by Western blot analysis and is shown in the lower panel. (TCV: turnip crinkle virus; CTLV: citrus tatter leaf virus; CP: coat protein; MP: movement protein; WB: western blot)

CTLV-CP and -MP did not directly bind with dsRNA and siRNA of GFP

To investigate if the CTLV CP and MP interact via direct binding with dsRNA and siRNA, RNA-protein pull-down assays were performed. Western blot analysis showed that the VSR controls TCV P38 and tomato bushy stunt virus (TBSV) P19 proteins, previously shown to interact with siRNA to suppress host RNA silencing (Incarbone and Dunoyer 2013; Vargason et al. 2003), were both pulled down by the dsRNA and siRNA of GFP, respectively (Figure 10a and 10b). However, CTLV-CP and CTLV-MP did not show any such interaction with either dsRNA or siRNA of GFP in the assays (Figure 10a and 10b).

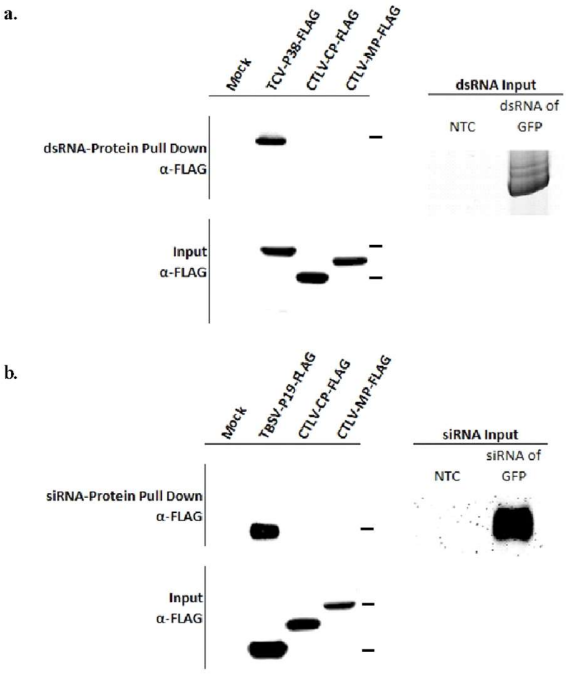

Fig. 10. Western blot analysis of RNA-protein pull-down assay to examine RNA binding capabilities of CTLV-CP and -MP with (a) double-stranded RNA (dsRNA) and (b) small interfering RNA (siRNA) of *GFP*. Inputs of dsRNA and siRNA were examined by polyacrylamide gel electrophoresis. (TCV: turnip crinkle virus; CTLV: citrus tatter leaf virus; TBSV: tomato bushy stunt virus; CP: coat protein; MP: movement protein)

Discussion

Viruses evolve and utilize silencing suppressors, VSRs, to counteract host antiviral RNA silencing by inhibiting or blocking such defense mechanisms at both local and systemic levels (Csorba et al. 2015; Ding 2010; Song et al. 2011; Wang et al. 2012; Burgyán and Havelda 2011). In this study, a series of different methodologies were employed for the identification and characterization of the VSRs of CTLV, an important citrus pathogen capable of inducing bud union crease on the widely commercially used trifoliate and citrange rootstocks (Calavan et al. 1963; Miyakawa et al. 1976).

During the molecular characterization of the two CTLV VSRs presented in this study, our approach indicated that RT-qPCR was highly compatible with the widely used *N. benthamiana* agroinfiltration assay while allowing a more accurate assessment of GFP relative expression levels in comparison to Northern blot hybridization.

The CTLV CP was proven to have silencing suppression activity in systemic tissues but at a low suppression rate (44%; Table 1). Viral CPs have multiple functions during virus infection, including virus entry, viral protein translation, replication, virus movement, transmission, and symptom development (Weber and Bujarski 2015). Previously, it has been reported that the ASGV CP, in addition to being expressed via a subgenomic

RNA (similar to CTLV), is essential for ASGV infectivity (Komatsu et al. 2012; Tatineni et al. 2009b). CTLV being a strain of ASGV, with a broad citrus host range, and with a high degree of sequence conservation (Tan et al. 2019), led to the hypothesis for this study that the CTLV CP could be a potential VSR. It is possible that the CP silencing suppression function might be established and manifest itself in response to a balance between the positive effects on the obligatory parasite virus life cycle and the negative effects on the host (Csorba et al. 2015). Our results implied that there might be trade-offs among different CTLV-CP functions that influence its silencing suppression activity.

The CTLV MP was confirmed as a local VSR with silencing suppression activity levels similar to those of CLBV-MP (Renovell et al. 2012). CTLV and CLBV both belong to the *Betaflexiviridae* family. Apple chlorotic leaf spot virus (ACLSV) is another *Betaflexiviridae* member with a movement protein demonstrating silencing suppression activity. However, the ACLSV MP is unable to suppress local silencing but can exert systemic silencing (Atabekova et al. 2023; Yaegashi et al. 2007). Based on our findings with the CTLV MP and earlier studies conducted with the CLBV MP, it is possible that the molecular machinery underlying silencing suppression induced by the MP of these two viruses may be different from that of ACLSV-MP. Overall, this and cited previous studies on *Betaflexiviridae* members suggest a trend that viruses within this family potentially use their MPs as VSRs despite their low sequence similarity (Atabekova et al. 2023). Further investigations are needed to help elucidate the molecular intricacies of suppression of host RNA silencing by these viruses. While previous studies showed that CLBV-MP had only local RNA silencing suppression activity (Renovell et al. 2012), in our experiments, a low suppression rate (15%) of systemic silencing activity was also detected (Table 1) for CLBV-MP which had relative expression levels similar to those of CMV-2b (Figure 3b).

The relative expression levels of CTLV-MP in systemic non-infiltrated leaves were significantly lower, more than 50% when compared to CMV-2b and CLBV-MP (Figure 3b). It has been reported that VSRs not only contribute to the suppression of host gene silencing but also interfere with host microRNA (miRNA) pathways regulating gene expression, affecting normal cell and plant growth (Liu et al. 2012; Wang et al. 2012). Therefore, it is possible that the observed suppression activity of the CTLV MP is due not only to its function in suppression of siRNA-mediated RNA silencing but also to its potential interference with host gene expression and disruption of miRNA functions, which may have affected the GFP expression levels.

The VSR activity of both CTLV-CP and -MP was also confirmed by agroinfiltration assays in wild-type *N. benthamiana* plants following expression with a PVX infectious vector in a virus-induced gene silencing (VIGS) background (Jones et al. 1999). In these experiments, CTLV-CP and CTLV-MP had dramatic effects on symptom development and PVX viral RNA accumulation in *N. benthamiana*. Both proteins acted as pathogenicity determinants to promote PVX infection, likely through their RNA silencing suppression activities (Qiao et al. 2013; Zhou et al. 2006). The frameshift mutant controls also proved that the silencing suppression activity was determined by the proteins themselves instead of their mRNA sequences.

The functionally active regions of the CTLV CP and MP were identified in this study. However, further experiments are needed to locate the specific domains, motifs or amino acid sites required for silencing suppression. Our co-immunoprecipitation experiments followed by mass spectrometry proteomics analysis (ten Have et al. 2011; Turriziani et al. 2016) did not identify direct interacting host proteins associated with the host RNA silencing pathway. Therefore, the CTLV VSRs may target other endogenous host regulators and factors to further modulate host antiviral defense indirectly (Csorba et al. 2015).

Instead of targeting proteins associated with the silencing pathway, some VSRs bind to RNA components such as long dsRNA or siRNA to suppress the antiviral defense response (Díaz-Pendón and Ding 2008; Csorba and Burgyán 2015; Pumplin and Voinnet 2013; Incarbone and Dunoyer 2013; Burgyán and Havelda 2011). The CTLV CP, as a systemic VSR, did not display any direct interaction with siRNAs, which can move systemically (Schwach et al. 2005; Martín-Hernández and Baulcombe 2008; Qu et al. 20051). This indicated that CTLV-CP could use indirect strategies to suppress systemic gene silencing. On the other hand, the results of the RIP and RNA-protein pull-down assays showed that the CTLV MP interacted with dsRNA indirectly which might be achieved with the help of a protein, a protein complex containing RNA binding domains, or by utilizing other indirect mechanisms to suppress host RNA silencing. This suggests that the CTLV MP might contribute to silencing suppression by preventing dsRNA from being processed by the host Dicer proteins.

Both the CTLV CP and MP are weak VSRs with low suppression rates, similar to the CLBV-MP VSR (Renovell et al. 2012). Viruses carrying weak VSRs tend to co-exist with their host rather than accumulate at high titers and cause severe damage or death to the infected plants (Renovell et al. 2012). The two identified VSRs could be some of the key factors responsible for the evolution and pathogenicity of the CTLV which only causes mild symptoms or remains symptomless on most of its wide range of hosts.

The potential for CTLV to cause serious problems to citrus production is a man-made situation where a CTLV-infected scion is grafted onto a trifoliate or trifoliate hybrid rootstock leading to bud union incompatibility, canopy decline, and tree death (Garnsey 1964; Calavan et al. 1963; Garnsey and Jones 1968; Roistacher 1991). It is unlikely that CTLV encountered a scion propagated onto a rootstock prior to the 19th century, when grafting was introduced as a standard procedure in commercial citrus groves. Moreover, the probability that a citrus tree was propagated onto a trifoliate rootstock before the 1950s is

even lower (Bitters 2021; Moreno et al. 2008; Mudge et al. 2009). Therefore, it is potentially feasible that the non-pathogenic equilibrium of CTLV in non-symptomatic citrus hosts was only recently disrupted by the rising rate of commercial citrus scion grafting onto trifoliate rootstocks. Although this theory needs substantiating with tangible research-based evidence, it is not the first case of such a situation occurring with a citrus virus. In the early 20th century, citrus tristeza virus (CTV) caused the most catastrophic virus epidemic in history directly linked to a specific scion-rootstock combination. More specifically, CTV is symptomless in most of its citrus hosts and only causes stem pitting and leaf symptoms in some sensitive species (Moreno et al. 2008; Roistacher 1991). However, when CTV encountered the man-made propagations of sweet orange (*C. sinensis* (L.) Osbeck) scions on sour orange (*C. aurantium* L.) rootstocks in the mid-1900s, the destructive tristeza quick decline disease emerged and killed millions of trees worldwide (Moreno et al. 2008).

Protecting the valuable trifoliate and trifoliate hybrid rootstocks from CTLV is of extreme importance for the global citriculture. Based on the past CTV epidemic (Moreno et al. 2008), it appears that CTLV has the potential to induce significant damage to the citrus industry since humans, as a key component of the plant disease tetrahedron (Zadoks and Schein 1979), have created an artificial monoculture environment with virus-sensitive host plants. Unlike CTV, CTLV does not appear to have a natural vector. Therefore, it is imperative that all phytosanitary measures for the use of pathogen-tested propagative materials be strictly enforced, thereby preventing spreading of CTLV (Fuchs et al. 2021; Gergerich et al. 2015). Similarly, the findings presented in this study represent key progress towards improving our understanding of the molecular interactions of CTLV with its hosts. Further studies could produce additional insights on its mode(s) for citrus infection, potentially leading to identification of critical points in the viral machinery which could act as targets for different intervention strategies facilitating disease mitigation, avoiding CTLV spread, economic and tree capital losses, and ultimately preserving the use of the trifoliate and trifoliate hybrid rootstocks in citriculture.

Acknowledgments

The authors acknowledge the Cahuilla people as the Traditional Custodians of the Land on which the experimental work was completed at UC Riverside. We thank Dr. Ma and Dr. Baulcombe for sharing the seeds of *N. benthamiana* wild-type and the transgenic line 16c. We are also grateful to all past and current CCPP personnel for their dedicated work and especially for creating and maintaining the CCPP disease bank and foundation materials. This project was supported by the USDA National Institute of Food and Agriculture Hatch project 1020106 and in part, by the National Clean Plant Network-USDA Animal and Plant Health Inspection Service (AP17PPQS&T00C118, AP18PPQS&T00C107, AP19PPQS&T00C148, and AP20PPQS&T00C049) and the Citrus Research Board project 6100 "Citrus Clonal Protection Program" awarded to G. Vidalakis.

References

Anandalakshmi R, Pruss GJ, Ge X, Marathe R, Mallory AC, Smith TH, et al. 1998. A viral suppressor of gene silencing in plants. Proceedings of the National Academy of Sciences of the United States of America, 95(22):13079-84.

Atabekova AK, Solovieva AD, Chergintsev DA, Solovyev AG, Morozov SY. 2023. Role of Plant Virus Movement Proteins in Suppression of Host RNAi Defense. International Journal of Molecular Sciences, 24(10):9049.

Baulcombe D. 2004. RNA silencing in plants. Nature, 431(7006):356-63.

Bewick V, Cheek L, Ball J. 2004. Statistics review 9: one-way analysis of variance. Critical care (London, England), 8(2):130-6.

Bitters WP. 2021. Citrus rootstocks: Their characters and reactions (an unpublished manuscript). Journal of Citrus Pathology, 8(1).

Bombarely A, Rosli HG, Vrebalov J, Moffett P, Mueller LA, Martin GB. 2012. A Draft Genome Sequence of Nicotiana benthamiana to Enhance Molecular Plant-Microbe Biology Research. Molecular Plant-Microbe Interactions, 25(12):1523-30.

Broadbent P, Dephoff CM, Gilkeson C. 1994. Detection of citrus tatter leaf virus in Australia. Australasian Plant Pathology, 23(1):20–4.

Burgyán J, Havelda Z. 2011. Viral suppressors of RNA silencing. Trends in Plant Science, 16(5):265-72.

Calavan EC, Christiansen DW, Roistacher CN. 1963. Symptoms associated with tatter-leaf virus infection of Troyer citrange rootstocks. Plant Disease Reporter, 47:971-5.

Calil IP, Fontes EP. 2017. Plant immunity against viruses: antiviral immune receptors in focus. Annals of Botany, 119(5):711-23.

Cook G, Steyn C, Breytenbach JHJ, de Bruyn R, Fourie PH. 2020. No detection of seed transmission of citrus tatter leaf virus in 'Meyer' lemon. Journal of Plant Diseases and Protection, 127(6):895-8.

Csorba T, Kontra L, Burgyán J. 2015. Viral silencing suppressors: Tools forged to fine-tune host-pathogen coexistence. Virology, 479-480:85-103.

da Graca JV. 1977. Citrus tatter leaf virus in South African Meyer lemon. Citrus and sub-tropical fruit journal.

da Graca JV, Skaria M. 1996. Citrus Tatter Leaf Virus in the Rio Grande Valley of South Texas. Proceedings of 13th Conference of International Organization of Citrus Virologists, 13(13). http://dx.doi.org/10.5070/C594n9s7kh Retrieved from https://escholarship.org/uc/item/94n9s7kh.

Díaz-Pendón JA, Ding SW. 2008. Direct and indirect roles of viral suppressors of RNA silencing in pathogenesis. Annual Review of Phytopathology, 46:303-26.

Ding SW. 2010. RNA-based antiviral immunity. Nature Reviews Immunology, 10(9):632-44.
Duncan DB. 1955. Multiple Range and Multiple F Tests. Biometrics, 11(1):1-42.
Earley KW, Haag JR, Pontes O, Opper K, Juehne T, Song K, et al. 2006. Gateway-compatible vectors for plant functional genomics and proteomics. The Plant Journal, 45(4):616-29.
Folimonova SY, Sun YD. 2022. Citrus tristeza virus: From pathogen to panacea. Annual Review of Virology, 9:417-35.
Fraser LR, Broadbent P. 1981. Virus and related diseases of citrus in New South Wales. Department of Agriculture New South Wales, p. 78.
Fuchs M, Almeyda CV, Al Rwahnih M, Atallah SS, Cieniewicz EJ, Farrar K, et al. 2021. Economic Studies Reinforce Efforts to Safeguard Specialty Crops in the United States. Plant Disease, 105(1):14-26.
Garcia-Ruiz H. 2019. Host factors against plant viruses. Molecular Plant Pathology, 20(11):1588-601.
Garnsey SM. 1964. Detection of tatter leaf virus of citrus in Florida. Florida State Horticultural Society, 77:106-9.
Garnsey SM, Jones JW. 1968. Relationship of symptoms to the presence of tatter-leaf virus in several citrus hosts. Proceedings of 4th Conference of International Organization of Citrus Virologists, 4(4). http://dx.doi.org/10.5070/C53nn328c4 Retrieved from https://escholarship.org/uc/item/3nn328c4.
Garnsey SM. 1970. Viruses in Florida's Meyer lemon trees and their effects on other citrus. Florida State Horticultural Society, 83:66–71.
Gergerich RC, Welliver RA, Gettys S, Osterbauer NK, Kamenidou S, Martin RR, et al. 2015. Safeguarding Fruit Crops in the Age of Agricultural Globalization. Plant Disease, 99(2):176-87.
Herron CM, Skaria M. 2000. Further Studies on Citrus Tatter Leaf Virus in Texas. Proceedings of 14th Conference of International Organization of Citrus Virologists, 14(14). http://dx.doi.org/10.5070/C51vf6401b Retrieved from https://escholarship.org/uc/item/1vf6401b.
Incarbone M, Dunoyer P. 2013. RNA silencing and its suppression: novel insights from in planta analyses. Trends in Plant Science, 18(7):382-92.
Inouye N, Maeda T, Mitsuhata K. 1979. Citrus tatter leaf virus isolated from lily. Annuals of the Phytopathological Society of Japan, 45:712-20.
Jones JD, Dangl JL. 2006. The plant immune system. Nature, 444(7117):323-9.
Jones L, Hamilton AJ, Voinnet O, Thomas CL, Maule AJ, Baulcombe DC. 1999. RNA–DNA Interactions and DNA Methylation in Post-Transcriptional Gene Silencing. The Plant Cell, 11(12):2291.
Khraiwesh B, Zhu J-K, Zhu J. 2012. Role of miRNAs and siRNAs in biotic and abiotic stress responses of plants. Biochimica et Biophysica Acta (BBA) - Gene Regulatory Mechanisms, 1819(2):137-48.
Komatsu K, Hirata H, Fukagawa T, Yamaji Y, Okano Y, Ishikawa K, et al. 2012. Infection of capilloviruses requires subgenomic RNAs whose transcription is controlled by promoter-like sequences conserved among flexiviruses. Virus Research, 167(1):8-15.
Li WX, Ding SW. 2001. Viral suppressors of RNA silencing. Current Opinion in Biotechnology, 12(2):150-4.
Liu D, Shi L, Han C, Yu J, Li D, Zhang Y. 2012. Validation of Reference Genes for Gene Expression Studies in Virus-Infected Nicotiana benthamiana Using Quantitative Real-Time PCR. PLOS ONE, 7(9):e46451.
Lucy AP, Guo HS, Li WX, Ding SW. 2000. Suppression of post-transcriptional gene silencing by a plant viral protein localized in the nucleus. The EMBO Journal, 19(7):1672-80.
Martín-Hernández AM, Baulcombe DC. 2008. Tobacco rattle virus 16-kilodalton protein encodes a suppressor of RNA silencing that allows transient viral entry in meristems. Journal of Virology, 82(8):4064-71.
Mérai Z, Kerényi Z, Kertész S, Magna M, Lakatos L, Silhavy D. 2006. Double-Stranded RNA Binding May Be a General Plant RNA Viral Strategy To Suppress RNA Silencing. Journal of Virology, 80(12):5747.
Miyakawa T, Matsui C. 1976. A Bud-Union Abnormality of Satusma Mandarin on *Poncirus Trifoliata* Rootstock in Japan. Proceedings of 7th Conference of International Organization of Citrus Virologists, 7(7). http://dx.doi.org/10.5070/C54kh677ch Retrieved from https://escholarship.org/uc/item/4kh677ch.
Miyakawa T. 1980. Occurrence and Varietal Distribution of Tatter Leaf-Citrange Stunt Virus and Its Effects on Japanese Citrus. Proceedings of 8th Conference of International Organization of Citrus Virologists, 8(8). http://dx.doi.org/10.5070/C59z21w7t7 Retrieved from https://escholarship.org/uc/item/9z21w7t7.
Miyakawa T, Tsuji M. 1988. The Association of Tatterleaf Virus with Budunion Crease of Trees on Trifoliate Orange Rootstock. Proceedings of 10th Conference of International Organization of Citrus Virologists, 10(10). http://dx.doi.org/10.5070/C57gv7436m Retrieved from https://escholarship.org/uc/item/7gv7436m.
Moffett P, Farnham G, Peart J, Baulcombe DC. 2002. Interaction between domains of a plant NBS-LRR protein in disease resistance-related cell death. The EMBO Journal, 21(17):4511-9.
Moreno P, Ambrós S, Albiach-Martí MR, Guerri J, Peña L. 2008. Citrus tristeza virus: a pathogen that changed the course of the citrus industry. Molecular Plant Pathology, 9(2):251-68.
Morton ER, Fuqua C. 2012. Laboratory maintenance of Agrobacterium. Current Protocols in Microbiology, 24(1):3D-1.
Mudge K, Janick J, Scofield S, Goldschmidt EE. 2009. A History of Grafting. Horticultural Reviews, p. 437-93.

Nelson RS, Citovsky V. 2005. Plant viruses. Invaders of cells and pirates of cellular pathways. Plant Physiology, 138(4):1809-14.

Nishio T, Kawai A, Kato M, Kobayashi T. 1982. A sap-transmissible closterovirus in citrus imported from China and Formosa. Research Bulletin of the Plant Protection Service (Japan).

Nishio T, Kawai, A., Takahashi, T., Namba, S., Yamashita, S. 1989. Purification and properties of citrus tatter leaf virus. Annals of the Phytopathological Society of Japan, 55:254-8.

Ohira K, Ito T, Kawai A, Namba S, Kusumi T, Tsuchizaki T. 1994. Nucleotide sequence of the 3'-terminal region of citrus tatter leaf virus RNA. Virus Genes, 8(2):169-72.

Ohira K, Namba S, Rozanov M, Kusumi T, Tsuchizaki T. 1995. Complete sequence of an infectious full-length cDNA clone of citrus tatter leaf capillovirus: comparative sequence analysis of capillovirus genomes. Journal of General Virology, 76(9):2305-9.

Pfaffl MW. 2001. A new mathematical model for relative quantification in real-time RT-PCR. Nucleic Acids Research, 29(9):e45-e45.

Pumplin N, Voinnet O. 2013. RNA silencing suppression by plant pathogens: defence, counter-defence and counter-counter-defence. Nature Reviews Microbiology, 11(11):745-60.

Qiao Y, Liu L, Xiong Q, Flores C, Wong J, Shi J, et al. 2013. Oomycete pathogens encode RNA silencing suppressors. Nature Genetics, 45(3):330-3.

Qu F, Ye X, Hou G, Sato S, Clemente TE, Morris TJ. 2005. RDR6 has a broad-spectrum but temperature-dependent antiviral defense role in Nicotiana benthamiana. Journal of Virology, 79(24):15209-17.

Rasmussen R. 2001. Quantification on the LightCycler. In: Meuer S, Wittwer C, Nakagawara K-I, editors. Rapid Cycle Real-Time PCR: Methods and Applications. Berlin, Heidelberg: Springer Berlin Heidelberg, p. 21-34.

Renovell Á, Vives MC, Ruiz-Ruiz S, Navarro L, Moreno P, Guerri J. 2012. The Citrus leaf blotch virus movement protein acts as silencing suppressor. Virus Genes, 44(1):131-40.

Roistacher CN. 1991. Graft-Transmissible Diseases of Citrus. In: Roistacher CN, editor. Handbook for detection and diagnosis of graft-transmissible diseases of citrus, p. 151-6.

Roose ML. 2014. Rootstocks. In: Ferguson L, Grafton-Cardwell EE, editors. Citrus Production Manual. University of California Agricultural and Natural Resources (UC ANR) Publication, 3539:95-105.

Roose ML, Gmitter FG, Lee RF, Hummer KE. 2015. Conservation of citrus germplasm: an international survey. In: Jaenicke H, Ashmore SE, Dulloo ME, Guarino L, Taylor M, editors. XXIX International Horticultural Congress on Horticulture: Sustaining Lives, Livelihoods and Landscapes (IHC2014): IV International Symposium on Plant Genetic Resources, p. 33-8.

Roth BM, Pruss GJ, Vance VB. 2004. Plant viral suppressors of RNA silencing. Virus Research, 102(1):97-108.

Ruiz MT, Voinnet O, Baulcombe DC. 1998. Initiation and maintenance of virus-induced gene silencing. The Plant Cell, 10(6):937-46.

Sanfaçon H. 2020. Modulation of disease severity by plant positive-strand RNA viruses: the complex interplay of multifunctional viral proteins, subviral RNAs and virus-associated RNAs with plant signaling pathways and defense responses. In: Carr JP, Roossinck MJ, editors. Advances in Virus Research. Academic Press, 107:87-131.

Schwach F, Vaistij FE, Jones L, Baulcombe DC. 2005. An RNA-dependent RNA polymerase prevents meristem invasion by potato virus X and is required for the activity but not the production of a systemic silencing signal. Plant Physiology, 138(4):1842-52.

Semancik JS, Weathers LG. 1965. Partial purification of a mechanically transmissible virus associate with tatter leaf of citrus. Phytopathology, 55:1354-8.

Song L, Gao S, Jiang W, Chen S, Liu Y, Zhou L, et al. 2011. Silencing suppressors: viral weapons for countering host cell defenses. Protein Cell, 2(4):273-81.

Su HJ, Cheon JU. 1984. Occurrence and distribution of tatter leaf-citrange stunt complex on Taiwanese citrus. Department of Entomology and Plant Pathology. National Taiwan University, p. 42–8.

Svec D, Tichopad A, Novosadova V, Pfaffl MW, Kubista M. 2015. How good is a PCR efficiency estimate: Recommendations for precise and robust qPCR efficiency assessments. Biomolecular Detection and Quantification, 3:9-16.

Tallarida RJ, Murray RB. 1987. Duncan Multiple Range Test. In: Tallarida RJ, Murray RB, editors. Manual of Pharmacologic Calculations with Computer Programs. New York, NY: Springer New York, p. 125-7.

Tan S-h, Osman F, Bodaghi S, Dang T, Greer G, Huang A, et al. 2019. Full genome characterization of 12 citrus tatter leaf virus isolates for the development of a detection assay. PLOS ONE, 14(10):e0223958.

Tanner JD, Kunta M, da Graca JV, Skaria M, Nelson SD. 2011. Evidence of a Low Rate of Seed Transmission of Citrus tatter leaf virus in Citrus. Proceedings of 18th Conference of International Organization of Citrus Virologists, 18(18). http://dx.doi.org/10.5070/C50b67q81h Retrieved from https://escholarship.org/uc/item/0b67q81h.

Tatineni S, Afunian MR, Hilf ME, Gowda S, Dawson WO, Garnsey SM. 2009. Molecular Characterization of Citrus tatter leaf virus Historically Associated with Meyer Lemon Trees: Complete Genome Sequence and Development of Biologically Active In Vitro Transcripts. Phytopathology, 99(4):423-31.

Tatineni S, Afunian MR, Gowda S, Hilf ME, Bar-Joseph M, Dawson WO. 2009b. Characterization of the 5′-and 3′-terminal subgenomic RNAs produced by a

capillovirus: Evidence for a CP subgenomic RNA. Virology, 385(2):521-8.
ten Have S, Boulon S, Ahmad Y, Lamond AI. 2011. Mass spectrometry-based immuno-precipitation proteomics – The user's guide. Proteomics, 11(6):1153-9.
Turriziani B, von Kriegsheim A, Pennington SR. 2016. Protein-Protein Interaction Detection Via Mass Spectrometry-Based Proteomics. In: Mirzaei H, Carrasco M, editors. Modern Proteomics – Sample Preparation, Analysis and Practical Applications. Cham: Springer International Publishing, p. 383-96.
Tuttle AR, Trahan ND, Son MS. 2021. Growth and maintenance of Escherichia coli laboratory strains. Current Protocols, 1(1):e20.
Vargason JM, Szittya G, Burgyán J, Hall TMT. 2003. Size Selective Recognition of siRNA by an RNA Silencing Suppressor. Cell, 115(7):799-811.
Wallace JM, Drake RJ. 1962. Tatter leaf, a previously undescribed virus effect on citrus. Plant Disease Reporter, 46:211-2.
Wroblewski T, Tomczak A, Michelmore R. 2005. Optimization of Agrobacterium-mediated transient assays of gene expression in lettuce, tomato and Arabidopsis. Plant Biotechnology Journal, 3(2):259-73.
Wang MB, Masuta C, Smith NA, Shimura H. 2012. RNA silencing and plant viral diseases. Molecular Plant-Microbe Interactions, 25(10):1275-85.
Weber PH, Bujarski JJ. 2015. Multiple functions of capsid proteins in (+) stranded RNA viruses during plant–virus interactions. Virus Research, 196:140-9.
Wu Q, Wang X, Ding SW. 2010. Viral Suppressors of RNA-Based Viral Immunity: Host Targets. Cell Host & Microbe, 8(1):12-5.
Yaegashi H, Takahashi T, Isogai M, Kobori T, Ohki S, Yoshikawa N. 2007. Apple chlorotic leaf spot virus 50 kDa movement protein acts as a suppressor of systemic silencing without interfering with local silencing in Nicotiana benthamiana. Journal of General Virology, 88(1):316-24.
Yoshikawa N, Imaizumi M, Takahashi T, Inouye N. 1993. Striking similarities between the nucleotide sequence and genome organization of citrus tatter leaf and apple stem grooving capilloviruses. Journal of General Virology, 74:2743-7.
Yoshikawa N. 2000. Apple stem grooving virus. CMI/AAB descriptions of plant viruses, p. 376.
Zadoks JC, Schein RD. 1979. Epidemiology and plant disease management. Oxford University Press Inc., New York, p. 427.
Zhang TM, Liang XY. 1988. Occurrence and detection of citrus tatter leaf virus (CTLV) in Huangyan, Zhejiang Province, China. Plant Disease, 72(6):543–5.
Zhou ZS, Dell'Orco M, Saldarelli P, Turturo C, Minafra A, Martelli GP. 2006. Identification of an RNA-silencing suppressor in the genome of Grapevine virus A. Journal of General Virology, 87:2387-95.